Cathodoluminescence investigations of GaInNAs on GaAs(111)*B*

J. Miguel-Sánchez[a)]
ISOM, Universidad Politécnica de Madrid, ETSI Telecomunicación, Ciudad Universitaria s/n, 28040 Madrid, Spain

U. Jahn
Paul-Drude-Institut für Festkörperelektronik, Hausvogteiplatz 5-7, 10117 Berlin, Germany

A. Guzmán and E. Muñoz
ISOM, Universidad Politécnica de Madrid, ESTI Telecomunicación, Ciudad Universitaria s/n, 28040 Madrid, Spain

(Received 27 July 2006; accepted 17 October 2006; published online 4 December 2006)

In this work, we present a detailed cathodoluminescence characterization of GaInNAs quantum wells grown on GaAs(111)*B*. As-grown and annealed InGaAs and GaInNAs quantum wells were maeasured and compared by spatially resolved cathodoluminescence at different photon energies. In the case of GaInNAs quantum wells, an increase of the luminescence intensity, a blueshift, and an increment of the modulation depth of intensity profiles were found after rapid thermal annealing cycles. The latter is caused by the presence of nonradiative areas above the GaInNAs quantum well due to stacking faults formed during the growth. © *2006 American Institute of Physics*. [DOI: 10.1063/1.2398919]

There has been an increasing interest of dilute nitrides, as found in many publications in recent past years.[1] The main interest of these materials and, in particular, of GaInNAs relies on their interesting physical properties: the addition of small quantities of the highly electronegative nitrogen atom to InGaAs layers strongly reduces the band gap. The high conduction band discontinuity with regard to GaAs and the possibility of growing virtually lattice-matched Al(Ga)As/GaAs reflectors make the GaInNAs material a good candidate for the development of GaAs based optoelectronic devices such as light emitting diodes and vertical cavity surface emitting lasers working in the wavelength range of optical telecommunications with very good thermal stability due to the strong electron confinement. Most of the work with this respect concerns GaInNAs grown on the more standard (100) GaAs orientation. Only a few publications were devoted to investigate dilute nitrides grown on higher index surfaces.[2–4]

These orientations, in particular, GaAs(111)*B*, show interesting properties. The presence of a piezoelectric field in strained heterostructures grown in this direction was theoretically predicted[5] and demonstrated in a variety of materials as, for example, the ternary InGaAs, which was incorporated as the active layer in a variety of electro-optical devices. In particular, low threshold InGaAs piezoelectric lasers were developed on GaAs(111)*B* in the past.[6] Additionally, a GaInNAs based laser diode was recently demonstrated on GaAs(111)*B* showing the viability for laser diode fabrication on this type of substrates.[7]

Although cathodoluminescence (CL) in a scanning electron microscope is a very powerful tool for the analysis of the material quality and structure,[8,9] only very few works are found in the literature devoted to CL investigations of dilute nitrides.[4,10,11] Previous work showed that a tunneling-assisted transport mechanism of carriers in dilute nitrides grown on both (100) and (111)*B* exists, different from the thermally activated carrier transport mechanism of GaAs/AlGaAs quantum wells (QWs).[4] In this work, we present a comprehensive CL characterization of GaInNAs QWs grown on GaAs(111)*B* to analyze the optical and structural qualities of such dilute nitride heterostructures. We studied comparatively equivalent InGaAs/GaAs and GaInNAs quantum wells grown on (111)*B* GaAs to extract the influence of N on the properties of such QWs.

The samples were grown by molecular-beam epitaxy on GaAs(111)*B* *n*+ (Si doped) misoriented substrate, using optimized growth conditions.[3,7,12] The samples were designed to form a *p*-*i*-*n* diode structure, with n^+ (2×10^{18} cm^{-3} Si doped) and p^+ (2×10^{18} cm^{-3} Be doped) regions, sandwiching an intrinsic 380-nm-thick GaAs layer. In the middle of the intrinsic layer, two 8-nm-thick quantum wells were grown consisting of an InGaAs layer with 24% In separated by a 40-nm-thick GaAs barrier and of an equivalent GaInNAs QW with nominal In and N contents of 24% and 2%, respectively. The cathodoluminescence measurements were carried out in a scanning electron microscope equipped with a liquid-He cooling stage for the samples, a computer-controlled integrated monochromator, and a near infrared detector. Annealing of the samples was carried out under an ultrapure N_2 atmosphere for 30 s at 850 °C with samples sandwiched between two dummy GaAs pieces.

In Figs. 1(a) and 1(b), the solid lines show the low temperature (12 K) cathodoluminescence spectra of the as-grown InGaAs and GaInNAs QWs, respectively. In the same figures, the dashed lines represent the CL spectra of the same QWs after a rapid thermal annealing (RTA) cycle of 30 s at 850 °C. RTA cycles are known to improve optical properties of dilute nitride QWs.[10,13] This is mainly due to a change of the bonding configuration of the nitrogen atoms during annealing, where the Ga–N bonds formed during the growth are reorganized and turn into In–N bonds.[10,13–15] As a result, we observe a narrowing of the luminescence spectra with increased intensity ($\approx\times6$), which are blueshifted by about 36 meV, as shown in Fig. 1(b). For the N-free InGaAs QW, however, the CL intensity is decreased after thermal cycling and a very subtle blueshift (4 meV) is observed, which is

a)FAX: +34 91 336 73 23; electronic mail: imiguel@die.upm.es

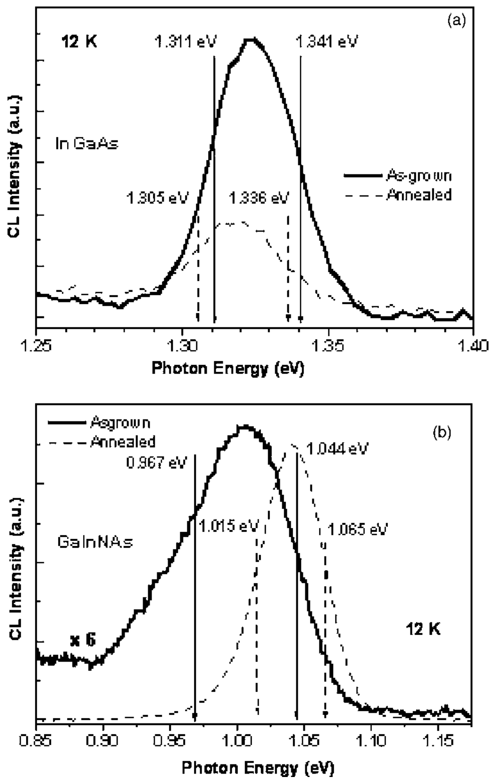

FIG. 1. Low temperature CL spectra of a 7 nm InGaAs QW (a) and a 7 nm GaInNAs QW (b), as-grown (solid lines) and after a RTA cycle (30 s at 850 °C, dashed lines). The arrows indicate the photon energies, at which the line scans of Fig. 2 were measured.

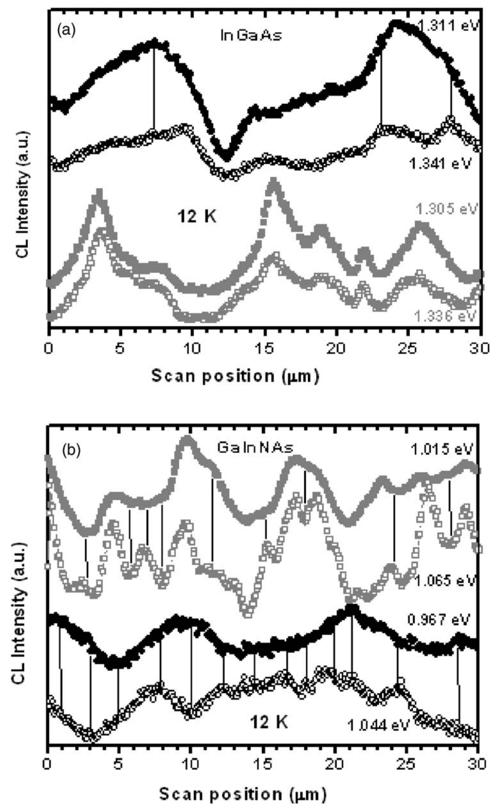

FIG. 2. Low temperature line profiles of the InGaAs (a) and GaInNAs (b) QWs of the CL intensities for values of the detection energies marked by the dashed arrows in Fig. 1. The black symbols show profiles of the as-grown QWs, and the gray symbols those of the annealed samples.

possibly due to a slight outdiffusion of indium and a respective broadening of the QW. As shown by high-resolution transmission electron microscopy (TEM), outdiffusion of In and N does not occur in GaInNAs QWs during the RTA cycle.[16]

CL mappings were used in the past to qualitatively analyze the optical emission of diluted nitrides.[4,11] To quantitatively analyze these mappings, we performed CL intensity line profiling for two different CL detection energies corresponding to the emission peaks of the InGaAs and GaInNAs QWs before and after annealing. These low temperature CL line scans are shown in Figs. 2(a) (InGaAs as grown and annealed) and 2(b) (GaInNAs as grown and annealed). The line profiles were measured for detection energies (E_d) set to the high- and low-energy sides of the CL spectra of the QWs as indicated by arrows in Figs. 1(a) and 1(b). CL line scans from the as-grown InGaAs QW represented by black symbols in Fig. 2(a) show significant intensity fluctuations. These fluctuations are similar for the low- and high-energy sides of the spectra, where no anticorrelation between the respective line scans is found. Only very slight short range deviations are shown for the high E_d CL intensity profile [cf. vertical lines in Fig. 2(a)]. These deviations are not found in the annealed InGaAs QW intensity profiles, as seen in the same figure. For the as-grown case of the GaInNAs QW—represented by black symbols in Fig. 2(b)—exhibiting the same indium content, the CL line profiles of the low- and high-energy sides are clearly anticorrelated in several areas of the measured profile. This stronger anticorrelation reflects fluctuations of the confinement energy of the GaInNAs QWs, which is probably caused by spatial fluctuations of the nitrogen composition in the QW after the growth. It is known that the addition of small quantities of N to InGaAs layers causes lateral fluctuations of the composition, which enhances the fluctuations of the confinement energy.

After annealing, as seen in Fig. 2(a), InGaAs line scans obtained for values of E_d at the low- and high-energy sides of the CL emission are still strongly correlated; the few fluctuations found in the as-grown sample at the high E_d not observed at low E_d were removed by annealing. The observed CL intensity fluctuations from the as-grown and annealed InGaAs QWs do not reflect energy variations: these are caused by general intensity variations of the whole spectrum probably due to an inhomogenous distribution of the nonradiative recombination centers, since no anticorrelations were found in its line scans. In the case of GaInNAs, we can quantitatively discuss the differences between the emission of the as-grown and annealed QWs by defining a difference $\delta(x)$ between the low- and high-energy CL intensities in the line scans [$I_{\mathrm{low}}(x)$ and $I_{\mathrm{high}}(x)$, respectively] at position x as $\delta(x)=|I_{\mathrm{low}}(x)-I_{\mathrm{high}}(x)|$. Taking its mean value $\bar{\delta}=(1/L)\int_0^L \delta(x)dx$ over the measurement distance L of the intensity profile, we obtain a quantity, which represents the value of the energy fluctuations in the QWs. This difference $\bar{\delta}_{\mathrm{GaInNAs}}$ is strongly increased after annealing (from $\bar{\delta}^{\text{as-grown}}_{\mathrm{GaInNAs}}=2240$ to $\bar{\delta}^{\text{annealed}}_{\mathrm{GaInNAs}}=22\,700$): CL intensity profiles at the low and high E_d still show relevant anticorrelations. Additionally, a stronger root-mean-square modulation depth is found. This modulation depth is defined by $\delta I_{\mathrm{rms}}/I=\sqrt{\langle(I-\langle I\rangle)^2\rangle}/\langle I\rangle$, where I is the CL intensity. As mentioned above for GaInNAs grown on GaAs (100), a bond reorganization after annealing is reported,[14,15] and a quantitative reduction of the CL intensity fluctuation was found.[11] Thus, a different mechanism must underlie, which is responsible for the strong

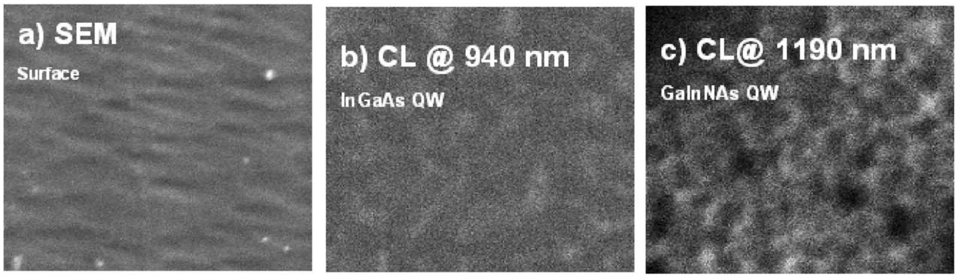

FIG. 3. $52\times45\ \mu m^2$ scanning electron microscopy (SEM) (a) and CL mappings of the double quantum well (DQW) sample for the InGaAs (b) and GaInNAs (c) detection energies.

increment of the modulation depth from $\delta I_{rms}^{as\text{-}grown}/I^{as\text{-}grown}=7\%$ to $\delta I_{rms}^{RTA}/I^{RTA}=19\%$ observed for the GaInNAs QWs grown on GaAs(111)*B*.

We explored therefore the complete CL mappings of the sample at the energy of the GaInNAs QW (1.015 eV). The surface morphology of the sample is shown in Fig. 3(a), and in more detail in Fig. 4(a). In this last image, the stepped morphology of the surface can clearly be recognized. The original steps with step edges perpendicular to the [2-1-1] direction are bunched and transformed into a zigzag morphology. The CL mappings of this sample for the InGaAs and GaInNAs peak energies are shown in Figs. 3(b) and 3(c), respectively. As seen in these mappings, there is no correlation between the surface morphology and the CL intensity distribution. The CL mapping of the InGaAs QW is composed of statistical fluctuations due to weak energy variations of the confinement potential[8] and speckle noise due to the measurement setup. The CL mapping of the GaInNAs QW is composed of statistical fluctuations, speckle, and particularly dark regions. The latter are randomly distributed. CL mappings at the energies marked by arrows in Fig. 1(b) exhibit the same dark regions (not shown). Figure 4(b) represents a more detailed CL image of a smaller region. The inset of this figure shows an augmented region of the mapping: the particularly dark regions reveal triangular shapes related to the underlying symmetry of the zinc-blende surface structure of the GaAs lattice in the [111] direction. For InGaAs, dark regions observed in CL mappings were found to be caused by the presence of extended lattice defects such as dislocations.[9] We relate these observed dark regions to nonradiative areas caused by tetrahedral stacking faults formed above the GaInNAs QW. These tetrahedral stacking faults have been measured by cross-section TEM and plain-view TEM (Ref. 17) for both the as-grown and annealed samples. The origin of the formation of these stacking faults is related to the presence of N_2 in the growth chamber.[17] Thus, these dark regions are responsible for the observed increment of the modulation depth of CL line scans, when we compare the as-grown and the annealed samples. These dark regions are not so clearly observed in the as-grown samples since the

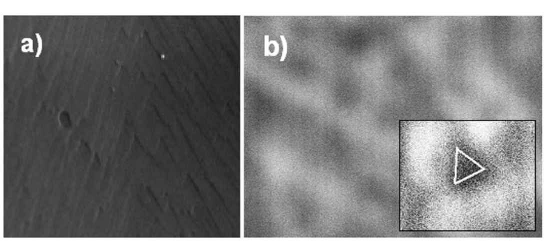

FIG. 4. High resolution SEM [$1\times1\ \mu m^2$ (a)] and CL mapping [$22.6\times16.8\ \mu m^2$ (b)] at the GaInNAs detection energy of the DQW sample. The inset shows an amplified area of the mapping showing triangular features. The white lines are drawn as a guide for the eyes.

QW CL intensity is much weaker than in the annealed samples. These CL line profiles show that although some of the areas of the QW are nonradiative the intensity of the CL spectrum is increased after annealing [cf. Fig. 2(b)], showing an improved quality of the GaInNAs/GaAs (111)*B* QWs.

In conclusion, we have presented a comprehensive CL characterization of GaInNAs QWs grown on GaAs(111)*B*. We have compared CL spectra of equivalent InGaAs and GaInNAs QWs before and after anneling. Low temperature GaInNAs QW CL intensity increased after annealing, due to bond reorganization, whereas the InGaAs QW CL intensity decreased possibly due to the QW outdiffusion. No anticorrelations were found in the as-grown and annealed InGaAs QW CL line scans. On the other hand, after annealing still some anticorrelations are found for GaInNAs QW CL intensity profiles at high and low E_d, showing an increased modulation depth. By measuring CL mappings we found triangular nonradiative areas on the GaInNAs QWs that we relate to stacking faults formed during growth over these QWs due to the presence of N.

This work has been supported by the European Union, Project No. IST-2000-26478-GINA1.5, and Spanish Ministerio de Educación y Ciencia.

[1] M. Kondow, K. Uomi, A. Niwa, T. Kitatani, S. Watahiki, and Y. Yazawa, Jpn. J. Appl. Phys., Part 1 **35**, 1273 (1996).
[2] S. Blanc, A. Arnoult, H. Carrère, and C. Fontaine, Physica E (Amsterdam) **17**, 252 (2003).
[3] J. Miguel-Sánchez, A. Guzmán, J. M. Ulloa, A. Hierro, and E. Muñoz, Appl. Phys. Lett. **84**, 2524 (2004).
[4] U. Jahn, S. Dhar, R. Hey, O. Brandt, J. Miguel-Sánchez, and A. Guzmán, Phys. Rev. B **73**, 125303 (2006).
[5] D. L. Smith, Solid State Commun. **57**, 919 (1986).
[6] I. W. Tao and W. I. Wang, Electron. Lett. **28**, 705 (1992).
[7] J. Miguel-Sánchez, A. Guzmán, J. M. Ulloa, M. Montes, A. Hierro, and E. Muñoz, IEEE Photonics Technol. Lett. **17**, 2271 (2005).
[8] E. Runge, J. Menniger, U. Jahn, R. Hey, and H. T. Grahn, Phys. Rev. B **52**, 12207 (1995).
[9] M. J. Romero, M. Gutiérrez, J. J. Sánchez, D. González, G. Aragón, I. Izpura, and R. García, Microelectron. J. **30**, 427 (1999).
[10] T. Kitatani, K. Nakahara, M. Kondow, K. Uomi, and T. Tanaka, J. Cryst. Growth **209**, 345 (2000).
[11] M. Kondow, T. Kitatani, and S. Shirakata, J. Phys.: Condens. Matter **16**, S3229 (2004).
[12] J. Miguel-Sánchez, M. Hopkinson, M. Gutiérrez, H. Y. Liu, P. Navaretti, A. Guzmán, J. M. Ulloa, and A. Hierro, J. Cryst. Growth **270**, 62 (2004).
[13] H. P. Xin, K. L. Kavanagh, and C. W. Tu, J. Cryst. Growth **208**, 145 (2000).
[14] S. Karinine, E. M. Pavelescu, J. Kontinnen, T. Jouhti, and M. Pessa, New J. Phys. **6**, 192 (2004).
[15] X. Liang, D. Jiang, B. Sun, L. Bian, Z. Pan, L. Li, and R. Wu, J. Cryst. Growth **243**, 261 (2002).
[16] A. Trampert, J.-M. Chauveau, K. H. Ploog, E. Tournié, and A. Guzmán, J. Vac. Sci. Technol. B **22**, 2195 (2004).
[17] E. Luna, A. Trampert, J. Miguel-Sánchez, A. Guzmán, and K. H. Ploog, J. Phys. Chem. Solids (to be published).